The use of agro-industrial residues of coffee (*Coffea arabica*) for the removal of mercury from water

Candelaria N. Tejada-Tovar[1] ✉ iD, María M. Rocha-Caicedo[2], Isabel C. Paz-Astudillo[2] iD

[1] Universidad de Cartagena, Faculty of Engineering, Department of Chemical Engineering,
Avenida Del Consulado 48-152, Cartagena 130014, Colombia

[2] Universidad del Tolima, Faculty of Agronomic Engineering, Ibagué, Colombia

Abstract: Contamination of water bodies by heavy metals is a continuously growing environmental issue. High concentrations of mercury (Hg) in river waters are a recognized environmental problem, because it is one of the most toxic heavy metal ions as it causes damage to the central nervous system. Its negative impact has led to the development of different methods for the treatment of effluents contaminated with Hg(II). The aim of this article is to evaluate the use of coffee (*Coffea arabica*) residues as adsorbent of Mercury in an aqueous solution. Four kinetic models, including intraparticle diffusion, pseudo-first-order, pseudo-second-order, and Elovich kinetic models were applied to explore the internal mechanism of mercury adsorption. Results indicate that the pseudo-first-order and pseudo-second-order models could accurately describe the adsorption process. It means that chemical adsorption play an important role in the adsorption of mercury by activated carbon. Meanwhile, the external mass transfer process is more effective in controlling the activated carbon mercury adsorption according to the fitting result of the pseudo-first-order model. The fitting to Langmuir's model suggested that the material surface is energetically homogeneous. The technique of contaminated biomass encapsulation proved to be safe for short-term disposal when metal recovery is not desired.

Keywords: agro-industrial residue, bioadsorption, encapsulation, heavy metals, isotherms

INTRODUCTION

Contamination of water bodies by heavy metals is a continuously growing environmental issue. Metals are introduced into aquatic systems naturally due to leaching from soils, rocks, and volcanic eruptions [Manirethan *et al.* 2019], or may also come from anthropogenic activities, such as agriculture, domestic waste, industry, and mining [Wang *et al.* 2016]. Nowadays, high contamination of inland waters occurs mainly due to mining tailings [Bisla *et al.* 2020].

High concentrations of metals such as mercury (Hg) in river waters are a recognised environmental problem. They are related to commercial gold extraction by small-scale miners [Lin *et al.* 2019]. Colombia releases an average of 75 Mg of mercury per year, making it number one in the world regarding the release of mercury per capita (1.6 g) [Cordy *et al.* 2011; Palacios-Torres

et al. 2018]. In the Colombian rivers, such as Cotuhé, Putumayo, San Jorge, and Caquetá, mercury concentrations have been found above 0.03 mg·dm^{-3} [Alcala-Orozco *et al.* 2019; Olivero-Verbel *et al.* 2016]. While the maximum concentration allowed by the Colombian Ministry of Environment and Sustainable Development (Ministerio de Ambiente y Desarrollo, MADS) in wastewater discharges from mining is 0.02 mg·dm^{-3} [MinAmbiente 2015], the World Health Organization (WHO) considers 0.001 mg·dm^{-3} an acceptable concentration in water designated for human consumption [WHO 2003]. Mercury is one of the most toxic heavy metal ions found at high concentrations in water. This metal can be found in nature in its inorganic forms: elemental mercury – Hg^0 or ionic – Hg(I) and Hg(II), and its organic forms: methylmercury – CH$_3$Hg, dimethylmercury – (CH$_3$)$_2$Hg, and phenylmercury – C$_6$H$_5$Hg [Bonilla Mejía 2020]. Although all chemical mercury species are considered hazardous

to humans, methylmercury is the most harmful compound. It can cause irreversible damage to the central nervous system [Iwai-Shimada et al. 2021]. For this reason, it caused a great concern in the scientific community, especially in countries where gold mining developed.

The negative impact of Hg(II) contamination on living organisms and the environment has necessitated the development of different methods for treatment of contaminated effluents, including precipitation, oxidation, reduction, ion exchange [Wang et al. 2020], filtration, electrochemical treatment, membrane technologies [Fard, Mehrnia 2017], and evaporative recovery [Huang et al. 2017]. However, these methods involve high operating costs and generate highly contaminated sludge. Additionally, bioadsorption using dry lignocellulosic biomass from lignocellulosic is applied as an alternative for the removal of heavy metals. The method has high removal efficiency, as well as possibility to reuse adsorbents and close the life cycle of residual materials [Arias Arias et al. 2017]. It was found that modification of corn-stalks, by introducing cyano, amino, amidoxime, and carboxyl groups onto its surface, can enhance mercury adsorption capacity on aqueous solution, with a maximum adsorption capacity of 1616 mg·g^{-1} [Wang et al. 2016].

On the other hand, a large part of the economy in the Department of Tolima is based on agriculture. Agricultural and agroindustrial practices generate residues rich in chemical compounds of interest, useful for the production of biomaterials with diverse applications and as a potential source of energy; however, the transformation of these residues into valuable products can improve the quality of life in the rural sector and increase the productivity and competitiveness of agroindustrial production chains [Andrade, Zapata 2019]. A particular case is the generation of pulp and mucilage during the conventional wet processing of coffee (*Coffea arabica*), when pulp and mucilage are not appropriately handled, unit contamination equivalent to 115 grams of chemical oxygen demand (*COD*) per kilogram of the coffee cherry is produced, of which 73.7% originates during depulping and pulp transport operations, and 26.3% during washing and classification [Andrade et al. 2018]. Pulp and mucilage represent respectively 72% and 28% [Atallah et al. 2018] of the contamination that reaches natural water courses, in such a proportion that one kilogram of processed fruit contaminates as much as the total volume of domestic wastewater generated by one inhabitant per day [Ordóñez Jurado et al. 2019].

Additionally, after applying the adsorption technique, bioadsorbents polluted with heavy metals need further disposal measures. In this sense, stabilisation/solidification with cement-based bricks is an option to encapsulate heavy metals by solidification [Roy, Stegemann 2017]. During encapsulation, heavy metal ions are sequestered in their crystalline form, and develop phases similar to zeolites and capillary pores. This reduces the activity and solubility of heavy metals [Wan et al. 2018]. Thus, the present report discusses the use of the residual coffee pulp as an adsorbent material for mercury in an aqueous solution, and it evaluates the effect of temperature and particle diameter on the adsorption capacity. The immobilisation of the metal was carried out by encapsulation in concrete matrices. Encapsulation of highly contaminated biomass with heavy metal ions was selected as a suitable alternative to solve disposal problems after the adsorption technique is applied.

MATERIALS AND METHODS

EXPERIMENTAL DESIGN

The study evaluated the effect of process temperature (*T*) and particle diameter (*Dp*) on the percentage of mercury adsorbed by the material. The study involved a 2^2 factorial experimental design with two replicates at each point and four central points. The minimum and maximum temperatures were 20 and 28°C, and the particle diameters were 0.4 and 0.8 mm. The central point corresponded to the conditions of 24°C and 0.6 mm. Operating conditions for the intervening variables are summarised in Table 1, based on previous studies carried out by the authors [Tejada et al. 2016; Tejada-Tovar et al. 2019].

Table 1. Operating conditions of mercury adsorption experiments on coffee pulp

Parameter	Value
pH	6
Initial mercury concentration in solution, C_0	0.2 mg·dm^{-3}
Contact time, t	4 h
Agitation rate	150 rpm
Solution volume, V	400 cm^3
Biomass mass / solution volume	5 g·dm^{-3}

Source: own study.

ADSORBENT PREPARATION

The coffee pulp (*Coffea arabica* L. var. 'Caturra') was obtained in the municipality of Líbano (Tolima) (latitude: 4.92199, longitude: –75.0614). The coffee pulp was selected, washed and chopped, then dried in an oven (Kryoven KO115) at 70 ±1°C for 24 h; it was then ground in a hammer mill (IKA MF10BS1) and manually sieved to separate it into specific particle sizes according to the experimental design. The biomass was characterised by bromatological analysis to quantify the presence of lignin, cellulose, and hemicellulose.

ADSORPTION TESTS

For the adsorption tests in a batch system, a stock synthetic solution of mercury was prepared at 0.2 mg·dm^{-3}; the pH was adjusted with hydrochloric acid (0.1 N). The Hg(II) solution was placed in contact with the bioadsorbent in a Lab Companion IST-3075 orbital shaker with permanent agitation for 4h. The final concentration of metal remaining in solution was determined by atomic absorption; the efficiency (*AY*) and adsorption capacity (q_e) were determined by Equations (1) and (2):

$$AY = \frac{(C_0 - C_f)}{C_0} \tag{1}$$

$$q_e = \frac{(C_0 - C_f)V}{m} \tag{2}$$

where: C_0 = initial concentration of metal in the solution (mg·dm^{-3}), C_f = final concentration of metal in the solution

(mg·dm^{-3}), V = volume of solution (dm^3), and m = mass of adsorbent (g).

The experimental data were analysed by ANOVA analysis of variance to determine the effect of temperature and particle diameter on the adsorption capacity of the material.

ADSORPTION ISOTHERM

The adsorption isotherm was performed by varying the initial metal concentration: 0.05, 0.15, 0.20, 0.25, 0.30 mg·dm^{-3}. The experiments were carried out at the temperature and particle diameter conditions that showed the highest adsorption efficiency during the adsorption test. The contact time was 6h; the other process conditions were kept constant according to Table 1.

Langmuir, Freundlich, Redlich–Peterson, and Sips models were fitted to the experimental data shown in Table 2. Thus, in order to determine which best describes the behaviour between the adsorbent and the adsorbate. The study used non-linear least-squares analysis, with σ^2 as a fitting parameter defined according to Equation (3).

$$\sigma^2 = \frac{\sum_{i=1}^{N} \left(y_{i,e} - y_{i,m}\right)^2}{N - p} \tag{3}$$

where: $y_{i,e}$ = experimental data, $y_{i,m}$ = data predicted by the model, N = number of experimental data and p = number of model parameters.

ADSORPTION KINETICS

The effect of time on the adsorption capacity of the adsorbent material was evaluated by performing a kinetic study [Ayub et al. 2019]. For this purpose, the adsorbent was placed in contact with the Hg(II) solution for 6 h, at the best conditions of temperature and particle diameter determined experimentally. The intervening variables were kept at the constant values established in Table 1. The experimental data obtained were fitted to the pseudo-first-order, pseudo-second-order, Elovich, and intraparticle diffusion models were fitted to the experimental data [Qiu et al. 2009]. The models are shown in Table 3.

Table 2. Isotherm models

Model	Equation	Parameter
Freundlich	$q_e = K_F C_e^{1/n}$	q_e (mg·g^{-1}) = amount of adsorbate adsorbed per gram of adsorbent at equilibrium K_F (dm^3·g^{-1}) = Freundlich's isothermal constant C_e (mg·dm^{-3}) = equilibrium adsorbate concentration n (–) = constant
Sips	$q_e = \dfrac{q_{ms} K_s C_e^{ms}}{1 + K_s C_e^{ms}}$	q_{ms} (mg·g^{-1}) = maximum adsorption capacity C_e^{ms} (mg·dm^{-3}) = equilibrium liquid phase concentration K_s (dm^3·g^{-1}) = Sips isotherm constant
Langmuir	$q_e = \dfrac{(Q_{max} K_L C_e)}{1 + K_L C_e}$	C_e (mg·dm^{-3}) = concentration of adsorbate in the equilibrium q_e (mg·g^{-1}) = amount of adsorbate adsorbed per gram of adsorbent at equilibrium Q_{max} (mg·g^{-1}) = coverage capacity in the monolayer K_L (–) = Langmuir isothermal constant
Redlich–Peterson	$q_e = \dfrac{A C_e}{1 + B C_e^{g}}$	C_e (mg·dm^{-3}) = concentration of adsorbate in the equilibrium A (–) and B (–) = Redlich–Peterson isotherm constants

Source: own elaboration.

Table 3. Kinetic adsorption models

Model	Equation	Parameter
Pseudo-first-order	$q_t = q_e\left(1 - e^{-k_1 t}\right)$	k_1 (min^{-1}) = Lagergren's constant q_e (mg·g^{-1}) = amount of contaminant adsorbed per unit mass in the equilibrium q_t (mg·g^{-1}) = amount of contaminant adsorbed per unit of mass at any time t t (min) = time
Pseudo-second-order	$q_t = \dfrac{t}{\frac{1}{k_2 \cdot q_e^2} + \frac{t}{q_e}}$	k_2 (g·mmol^{-1}·min^{-1}) = second order reaction speed coefficient q_e (mg·g^{-1}) = amount of contaminant adsorbed per unit mass in the equilibrium q_t (mg·g^{-1}) = amount of contaminant adsorbed per unit of mass at any time t t (min) = time
Elovich	$q_t = \dfrac{1}{\beta}\ln(\alpha\beta) + \dfrac{1}{\beta}\ln(t)$	α (mg·g^{-1}·min^{-1}) = initial adsorption rate β (g·mg^{-1}) = desorption constant related to surface range and activation energy for chemisorption q_t (mg·g^{-1}) = the amount of chemisorption gas in a time t t (min) = time
Intraparticle diffusion	$q_t = k_3 t^{0.5}$	t (min) = time q_t (mg·g^{-1}) = the amount of chemisorption gas in a time t k_3 (g·mg^{-1}·min^{-1}) = intraparticle diffusion rate constant

Source: own elaboration.

THERMODYNAMIC PARAMETERS

The feasibility of the adsorption process of Hg(II) on coffee pulp was estimated together with spontaneity, type of adsorption, and the effect of temperature on it, by determining the change in the standard Gibbs free energy ($\Delta G°$), standard enthalpy ($\Delta H°$) and the standard entropy ($\Delta S°$). For this purpose, the Van 't Hoff graphical method was applied, using Equations (4)–(6):

$$K_c = \frac{q_e}{C_e} \tag{4}$$

$$\Delta G° = -RT \cdot \ln K_c \tag{5}$$

$$\ln K_c = \frac{-\Delta H°}{RT} + \frac{\Delta S°}{R} \tag{6}$$

where: K_c = equilibrium constant, which represents the concentration of the solid phase at equilibrium (mg·g^{-1}), C_e = concentration at equilibrium (mg·g^{-1}), R = ideal gas constant 8.314 J·mol^{-1}·K^{-1}, and T = absolute temperature (K) [ZHAO *et al.* 2019].

The ($\Delta H°$) and ($\Delta S°$) are determined from the slope and y-axis intersection of ln K_c vs T^{-1}, respectively.

DISPOSAL OF METAL-CONTAMINATED RESIDUES

In order to properly dispose of the contaminated waste, ~100 g of the biomass with adsorbed metal was encapsulated in concrete blocks. A mixture of portland cement (32.4%), sand (25.9%), and gravel (41.7%) were used to manually produce each block in PVC pipes (17.78 cm in diameter and 30 cm in length). Initially, the concrete was poured up to half of the tube, then the contaminated biomass was added and then filled with the mixture. The blocks were left to set for 28 days. After, a leachate test was performed on the previously crushed blocks. For the leachate test was a mixture of sulphuric acid and nitric acid, prepared in a ratio 60/40%w in 1 dm^3 of distilled water at pH 4. Then 12 g of the sample (crushed block) and 250 cm^3 of the fluid (acid mixture) were taken and put in contact for 20 h under 115 rpm agitation. Once the contact time was over, the sample was filtered, and the liquid phase was analysed by atomic absorption [VILLABONA-ORTÍZ *et al.* 2018].

RESULTS AND DISCUSSION

QUANTIFICATION OF LIGNOCELLULOSIC COMPONENTS

Figure 1 shows the determination of the lignocellulosic components in the adsorbent material obtained from coffee pulp (*Coffea arabica* var. 'Caturra'). Its high percentage of cellulose and hemicellulose is evident. These are polymeric compounds with the capacity to adsorb metal ions because these polymers are known for the large amount of hydroxyl, carboxyl, and phenol groups that can favour the adsorption of heavy metals [LAWAL *et al.* 2017]. The presence of these compounds in the coffee structure suggests that mercury adsorption into the biomass might happened by ion exchange, micro-precipitation, complexation and coordination owing to the presence of functional groups [LI *et al.* 2017]. Thus, it involves the cation exchange mechanism and microprecipitation [PARK *et al.* 2019].
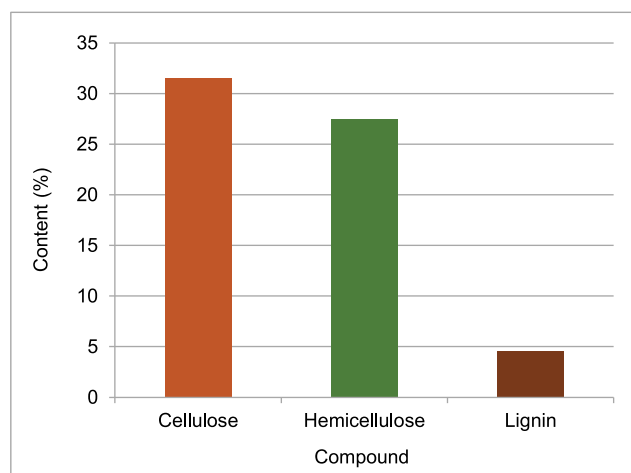

Fig. 1. Analysis of lignocellulosic components in the material based on coffee pulp; source: own study

EFFECT OF TEMPERATURE AND PARTICLE DIAMETER

The removal efficiency and adsorption capacity of Hg(II) on coffee pulp is shown in Table 2. Values between 0.038 and 0.040 mg·g^{-1} were obtained with efficiencies between 94 and 98%, with no direct dependence on temperature and particle diameter in the range of values studied, as confirmed by the analysis of variance (Tab. 4).

Table 4. Analysis of variance of Hg(II) adsorption on coffee pulp

Variation source	SS	MS	F-value	$F_{\alpha\,=\,0.05,1/11}$
Temperature	4.65	4.651	2.21	5.59
Particle diameter	4.65	4.651	2.21	5.59
Interaction	0.15	0.151	0.07	5.59
Curvature	0.57	0.570	0.27	5.59
Error	14.73	2.104	–	–
Total	**24.75**	–	–	–

Explanations: *SS* = statistical significance, *MS* = mean square, *F*-value = ratio of two variances, or technically, two mean squares.
Source: own study.

However, theory indicates that adsorption is a process influenced by mass and heat transfer [EL ASS 2018], where the surface area, and therefore the particle diameter, play an essential role in the provision of active sites. Temperature affects the spontaneity of the process, favouring the adsorption or desorption of the metal. Therefore, the results of the analysis of variance with the high adsorption results led to a conclusion that the range of the selected variables is within the optimal region of temperature and particle diameter to carry out the process, with the possibility of decreasing the metal concentration in water to values close to the maximum allowed in effluents (0.002 mg·dm^{-3}).

THERMODYNAMIC PARAMETERS

It is established that the removal of Hg(II) involves exothermic adsorption due to a negative $\Delta H°$ (see Tab. 5). Thus energy is released during the formation of bonds between ions and active

Table 5. Thermodynamic parameters of Hg(II) adsorption on coffee pulp

T (K)	$\Delta G°$ (J·mol^{-1})	$\Delta H°$ (J·mol^{-1})	$\Delta S°$ (J·mol·K^{-1})
293	4258.03479	–42292.469	–160.704
297	6607.89703	–	–
301	5512.72509	–	–

Explanations: T = absolute temperature, $\Delta G°$ = standard Gibbs free energy, $\Delta H°$= standard enthalpy, $\Delta S°$ = standard entropy.
Source: own study.

functional groups on the adsorbent [SALEH *et al.* 2017]. In addition, according to its value, chemisorption is suggested as a controlling mechanism during the process [RABIE *et al.* 2019]. Positive values of $\Delta G°$ indicate that the process is not spontaneous, and its increase with temperature makes it energetically more favourable [AL-GHOUTI *et al.* 2019]. The negative value of $\Delta S°$ suggests a decrease in the randomness in the solution/interface of the coffee pulp during the adsorption of Hg(II) in pores of the material, as well as spontaneity of the process and its low capacity [SHEN *et al.* 2018].

ADSORPTION EQUILIBRIUM

The metal concentration in the liquid and in the material when the equilibrium state at 20°C is reached described by the adsorption isotherm is shown in Figure 2. Similarly, the graphical representation of Langmuir, Freundlich, Redlich–Peterson, and Sips models can be observed.
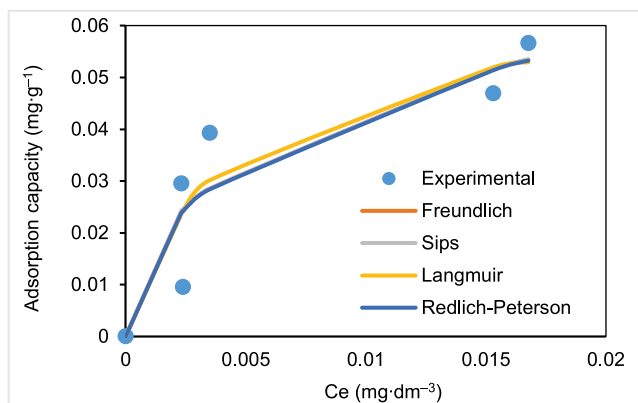
Fig. 2. Model fitting of Hg(II) adsorption isotherms on coffee pulp at 20°C; C_e = the concentration at equilibrium (mg·g^{-1}); source: own study

According to the results (Tab. 6), the fitting of the experimental data to the models was low, with a minimum variance of 0.00012 that corresponds to the Langmuir model with a maximum adsorption capacity of 0.066 mg·g^{-1}. According to the above, it is assumed that the material surface is homogeneous and that adsorption occurs in a monolayer, with a finite number of identical and specific adsorption sites, energetically equivalent and with no appreciable interaction between molecules [MORA ALVAREZ *et al.* 2018]. Previous studies have reported Langmuir q_{max} values of 32.6 mg·g^{-1} on dry biomass of *Chlorella vulgaris* at an initial concentration of Hg(II) between 11 and 90 mg·dm^{-3} [SOLISIO *et al.* 2019], 11.91 mg·g^{-1} using residual rose biomass with

Table 6. Fitting parameters of Hg(II) adsorption on the coffee pulp to isotherm models

Model	Parameter	Value	Model variance, σ^2
Freundlich	K_F	0.275	1.33e–4
	n	2.495	
Sips	q_{ms}	195.71	1.99e–4
	K_s	0.001	
	m_s	0.401	
Langmuir	Q_{max}	0.066	1.23e–4
	K_L	239.645	
Redlich–Peterson	A	120.463	1.99e–4
	B	477.693	
	q_e	0.626	

Explanation: all parameters are explained in p. 166.
Source: own study.

initial concentrations between 10 and 100 mg·dm^{-3} [AMAN *et al.* 2018], and 212.6 mg·g^{-1} using yucca shells modified with magnetic nanoparticles coated with organic amino ligands [MARIMÓN-BOLÍVAR *et al.* 2018].

ADSORPTION KINETICS

The fitting to the pseudo-first-order, pseudo-second-order, Elovich, and intraparticle diffusion models of Hg(II) adsorption kinetics on coffee pulp is shown in Figure 3. Rapid adsorption is observed in the first 40 min of the process, and equilibrium is reached at approximately 90 min of contact between the solution and the adsorbent; the rapid adsorption observed at the beginning of the removal is due to the availability of active sites on the surface of the bioadsorbent, which were occupied by ions as the contact time elapsed [ZHOU *et al.* 2017]. These results coincide with those reported for the removal of Hg(II) on biosynthesised melanin-coated PVDF membranes [MANIRETHAN *et al.* 2019]. When using cellulose nanofibrils extracted from rice straw, as in the present study, the adsorption capacity (q) increases with the increase in concentration of Hg(II) ions and after a 40 min contact time until reaching equilibrium [BISLA *et al.* 2020].
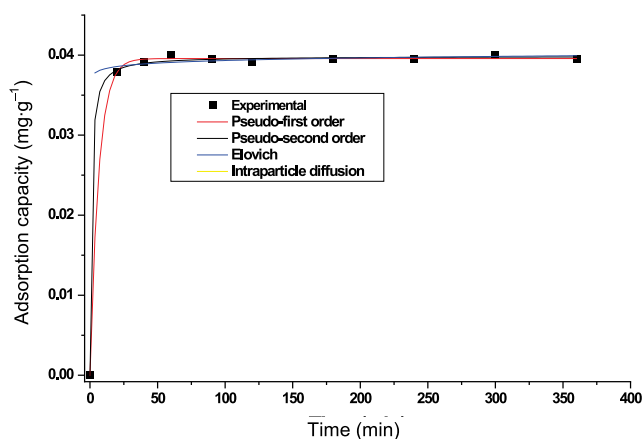
Fig. 3. Fitting to kinetic models of Hg(II) adsorption on coffee pulp at 20°C; source: own study

The adsorption capacity of adsorbent for Hg(II) ions depends upon its chemical and physical properties, and the hydrolysis capacity of metal ions [ZHANG *et al.* 2012].

According to Table 7 and Figure 3, it is established that the kinetic models that best fit the experimental data were the pseudo-second-order and pseudo-first-order models; this suggests that the process is carried out by chemisorption, i.e. there is an ion exchange between the Hg^{2+} cations and the surface functional groups of the biomass (mainly carbonyl and hydroxyl groups of cellulose and hemicellulose) [WANG *et al.* 2019]. This fact is due to the formation of chemical bonds between adsorbent and adsorbate on the surface [DOKE, KHAN 2017]. The adjustment to the pseudo-first-order meant that the external mass transfer process is more effective in terms of controlling the mercury adsorption process using coffee residues [WANG *et al.* 2019].

Table 7. Adjustment parameters of the kinetic models of Hg(II) adsorption

Kinetic model	Parameter	Value
Pseudo-first-order	q_{e1} (mg·g^{-1})	0.039
	k_1 (min^{-1})	1.0428
	R^2	0.9977
	SS	3.177e–6
Pseudo-second-order	k_2 (g mg^{-1} min^{-1})	45.256
	q_{e2} (mg·g^{-1})	0.04
	R^2	0.999
	SS	0.0046
Elovich	β	21.4550
	α	1.216e–5
	R^2	0.9807
	SS	0.0139
Intraparticle diffusion	k_3	0.00292
	R^2	0.3983
	SS	0.0019

Explanation: R^2 = determination coefficient, SS is explained in Tab. 4 and the other parameters are explained in p. 166.
Source: own study.

FINAL DISPOSAL OF BIOMASS CONTAMINATED WITH METAL

The atomic absorption test performed on the leachate from the block fragments indicated an imperceptible amount of metal in the liquid, with the lower detection limit of the equipment being 0.002 mg·dm^{-3}. This suggests that the concrete encapsulation method for the disposal of contaminated biomass is safe. These results could be attributed to the formation of bonds between heavy metals and oxides found in cement, such as CaO, Al_2O_3, and Fe_2O_3 [DU *et al.* 2014]. It is expected that these results are maintained in the long run regardless environmental and storage conditions. It is considered essential to perform a shelf-life study on the blocks to confirm the effectiveness of the method when metal recovery is not desired. The encapsulation of heavy metals in blocks facilitates the final treatment and fill a knowledge gap regarding the contaminated biomass and leaching of mercury from a biomass structure, and bricks.

CONCLUSIONS

The results show that residual coffee pulp is a promising adsorbent of Hg(II) at low concentrations, similar to those reported for contamination in water sources. It is expected that high adsorption percentages are reproducible with real water due to the interaction of the metal with other compounds that facilitate the adsorption process. It is also established that (i) efficiency and adsorption capacity of the biomaterial does not depend on temperature and particle diameter at the conditions evaluated in the present study; (ii) from the thermodynamic study, it is established that the Hg(II) removal process is exothermic; its mechanism is controlled by chemisorption, it is not spontaneous and energetically more favourable as the temperature increases; (iii) experimental adsorption equilibrium data were fitted by the Langmuir model, thus demonstrating that the material's surface is energetically homogeneous; (iv) kinetic study indicated that equilibrium is reached after approximately 90 min; the kinetic model that best fitted the experimental data is the pseudo-second-order model. This shows that the process is generated by ion exchange between the Hg(II) cations the surface functional groups of the biomass; (v) the technique of encapsulation of the contaminated biomass proved to be safe for short-term disposal when metal recovery is not desired.

ACKNOWLEDGMENTS

FUNDING

REFERENCES

AL-GHOUTI M.A., DA'ANA D., ABU-DIEYEH M., KHRAISHEH M. 2019. Adsorptive removal of mercury from water by adsorbents derived from date pits. Scientific Reports. Vol. 9(1) p. 1–15. DOI 10.1038/s41598-019-51594-y.

ALCALA-OROZCO M., CABALLERO-GALLARDO K., OLIVERO-VERBEL J. 2019. Mercury exposure assessment in indigenous communities from Tarapaca village, Cotuhe and Putumayo Rivers, Colombian Amazon. Environmental Science and Pollution Research. Vol. 26 (36) p. 36458–36467. DOI 10.1007/s11356-019-06620-x.

AMAN A., AHMED D., ASAD N., MASIH R., ABD UR RAHMAN H.M. 2018. Rose biomass as a potential biosorbent to remove chromium, mercury and zinc from contaminated waters. International Journal of Environmental Studies. Vol. 75(5) p. 774–787. DOI 10.1080/00207233.2018.1429130.

ANDRADE H.J., ZAPATA P.C. 2019. Mitigation of climate change of coffee production systems in Cundinamarca, Colombia. Floresta e Ambiente. Vol. 26(3) p. 1–11. DOI 10.1590/2179-8087.012618.

ANDRADE H.J.C., SEGURA M.A., FERIA M., SUÁREZ W. 2018. Above-ground biomass models for coffee bushes (*Coffea arabica* L.) in Líbano, Tolima, Colombia. Agroforestry Systems. Vol. 92(3) p. 775–784. DOI 10.1007/s10457-016-0047-4.

ARIAS ARIAS F.E., BENEDUCI A., CHIDICHIMO F., FURIA E., STRAFACE S. 2017. Study of the adsorption of mercury (II) on lignocellulosic materials under static and dynamic conditions. Chemosphere. Vol. 180 p. 11–23. DOI 10.1016/j.chemosphere.2017.03.137.

ATALLAH S.S., GÓMEZ M.I., JARAMILLO J. 2018. A bioeconomic model of ecosystem services provision: Coffee berry borer and shade-grown coffee in Colombia. Ecological Economics. Vol. 144 p. 129–138. DOI 10.1016/j.ecolecon.2017.08.002.

AYUB S., MOHAMMADI A.A., YOUSEFI M., CHANGANI F. 2019. Performance evaluation of agro-based adsorbents for the removal of cadmium from wastewater. Desalination and Water Treatment. Vol. 142 p. 293–299. DOI 10.5004/dwt.2019.23455.

BISLA V., RATTAN G., SINGHAL S., KAUSHIK A. 2020. Green and novel adsorbent from rice straw extracted cellulose for efficient adsorption of Hg (II) ions in an aqueous medium. International Journal of Biological Macromolecules. Vol. 161 p. 194–203. DOI 10.1016/j.ijbiomac.2020.06.035.

BONILLA MEJÍA L. 2020. Mining and human capital accumulation: Evidence from the Colombian gold rush. Journal of Development Economics. Vol. 145, 102471. DOI 10.1016/j.jdeveco.2020.102471.

CORDY P., VEIGA M.M., SALIH I., AL-SAADI S., CONSOLE S., GARCIA O., MESA L.A., VELÁSQUEZ-LÓPEZ P.C., ROESER M. 2011. Mercury contamination from artisanal gold mining in Antioquia, Colombia: The world's highest per capita mercury pollution. Science of the Total Environment. Vol. 410–411 p. 154–160. DOI 10.1016/j.scitotenv.2011.09.006.

DOKE K.M., KHAN E.M. 2017. Equilibrium, kinetic and diffusion mechanism of Cr(VI) adsorption onto activated carbon derived from wood apple shell. Arabian Journal of Chemistry. Vol. 10. Suppl. 1 p. S252–S260. DOI 10.1016/j.arabjc.2012.07.031.

DU Y., WEI M., REDDY K., LIU Z., JIN F. 2014. Effect of acid rain pH on leaching behavior of cement stabilized lead-contaminated soil. Journal of Hazardous Materials. Vol. 271 p. 131–140. DOI 10.1016/j.jhazmat.2014.02.002.

EL ASS K. 2018. Adsorption of cadmium and copper onto natural clay: Isotherm, kinetic and thermodynamic studies. Global Nest Journal. Vol. 20(2) p. 198–207. DOI 10.30955/gnj.002352.

FARD G.H., MEHRNIA M.R. 2017. Investigation of mercury removal by micro-algae dynamic membrane bioreactor from simulated dental waste water. Journal of Environmental Chemical Engineering. Vol. 5(1) p. 366–372. DOI 10.1016/j.jece.2016.11.031.

HUANG N., ZHAI L., XU H., JIANG D. 2017. Stable covalent organic frameworks for exceptional mercury removal from aqueous solutions. Journal of the American Chemical Society. Vol. 139(6) p. 2428–2434. DOI 10.1021/jacs.6b12328.

IWAI-SHIMADA M., KOBAYASHI Y., ISOBE T., NAKAYAMA S.F., SEKIYAMA M., TANIGUCHI Y., ..., SHIMONO M. 2021. Comparison of simultaneous quantitative analysis of methylmercury and inorganic mercury in cord blood using LC-ICP-MS and LC-CVAFS: The pilot study of the Japan environment and children's study. Toxics. Vol. 9(4) p. 82. DOI 10.3390/toxics9040082.

LAWAL O.S., AYANDA O.S., RABIU O.O., ADEBOWALE K.O. 2017. Application of black walnut (Juglans nigra) husk for the removal of lead (II) ion from aqueous solution. Water Science and Technology. Vol. 75(10) p. 2454–2464. DOI 10.2166/wst.2017.125.

LI G., WANG S., WU Q., WANG F., DING D., SHEN B. 2017. Mechanism identification of temperature influence on mercury adsorption capacity of different halides modified bio-chars. Chemical Engineering Journal. Vol. 315 p. 251–261. DOI 10.1016/J.CEJ.2017.01.030.

LIN G., HU T., WANG S., XIE T., ZHANG L., CHENG S., FU L., XIONG C. 2019. Selective removal behavior and mechanism of trace Hg(II) using modified corn husk leaves. Chemosphere. Vol. 225 p. 65–72. DOI 10.1016/j.chemosphere.2019.03.006.

MANIRETHAN V., GUPTA N., BALAKRISHNAN R.M., RAVAL K. 2019. Batch and continuous studies on the removal of heavy metals from aqueous solution using biosynthesised melanin-coated PVDF membranes. Environmental Science and Pollution Research. Vol. 27 p. 24723–24737. DOI 10.1007/s11356-019-06310-8.

MARIMÓN-BOLÍVAR W., TEJEDA-BENÍTEZ L., HERRERA A.P. 2018. Removal of mercury (II) from water using magnetic nanoparticles coated with amino organic ligands and yam peel biomass. Environmental Nanotechnology, Monitoring and Management. Vol. 10 p. 486–493. DOI 10.1016/j.enmm.2018.10.001.

MinAmbiente 2015. Resolución 0631 de 2015 (17 Mar) Por la cual se establecen los parámetros y los valores límites máximos permisibles en los vertimientos puntuales a cuerpos de aguas superficiales y a los sistemas de alcantarillado público y se dictan otras disposiciones. Bogotá. Ministerio de Ambiente y Desarrollo Sostenible pp. 62. The Resolución is available at: https://www.minambiente.gov.co/documento-normativa/resolucion-631-de-2015/

MORA ALVAREZ N.M., PASTRANA J.M., LAGOS Y., LOZADA J.J. 2018. Evaluation of mercury (Hg^{2+}) adsorption capacity using exhausted coffee waste. Sustainable Chemistry and Pharmacy. Vol. 10 p. 60–70. DOI 10.1016/j.scp.2018.09.004.

OLIVERO-VERBEL J., CARRANZA-LOPEZ L., CABALLERO-GALLARDO K., RIPOLL-ARBOLEDA A., MUÑOZ-SOSA D. 2016. Human exposure and risk assessment associated with mercury pollution in the Caqueta River, Colombian Amazon. Environmental Science and Pollution Research. Vol. 23(20) p. 20761–20771. DOI 10.1007/s11356-016-7255-3.

ORDÓÑEZ JURADO H.R., NAVIA ESTRADA J.F., BALLESTEROS POSSÚ W. 2019. Tipificación de sistemas de producción de café en La Unión Nariño, Colombia [Typification of coffee production systems in La Unión Nariño, Colombia]. Temas Agrarios. Vol. 24(1) p. 53–65. DOI 10.21897/rta.v24i1.1779.

PALACIOS-TORRES Y., CABALLERO-GALLARDO K., OLIVERO-VERBEL J. 2018. Mercury pollution by gold mining in a global biodiversity hotspot, the Choco biogeographic region, Colombia. Chemosphere. Vol. 193 p. 421–430. DOI 10.1016/j.chemosphere.2017.10.160.

PARK J.H., WANG J.J., ZHOU B., MIKHAEL J.E.R., DELAUNE R.D. 2019. Removing mercury from aqueous solution using sulfurized biochar and associated mechanisms. Environmental Pollution. Vol. 244 p. 627–635. DOI 10.1016/J.ENVPOL.2018.10.069.

QIU H., LV L., PAN B.C., ZHANG Q.J., ZHANG W.M., ZHANG Q.X. 2009. Critical review in adsorption kinetic models. Journal of Zhejiang University: Science A. Vol. 10(5) p. 716–724. DOI 10.1631/jzus.A0820524.

RABIE A.M., ABD EL-SALAM H.M., BETIHA M.A., EL-MAGHRABI H.H., AMAN D. 2019. Mercury removal from aqueous solution via functionalized mesoporous silica nanoparticles with the amine compound. Egyptian Journal of Petroleum. Vol. 28(3) p. 289–296. DOI 10.1016/j.ejpe.2019.07.003.

Roy A., Stegemann J. 2017. Nickel speciation in cement-stabilized/solidified metal treatment filtercakes. Journal of Hazardous Materials. Vol. 321 p. 353–361. DOI 10.1016/j.jhazmat.2016.09.027.

Saleh T.A., Sari A., Tuzen M. 2017. Optimization of parameters with experimental design for the adsorption of mercury using polyethylenimine modified-activated carbon. Journal of Environmental Chemical Engineering. Vol. 5(1) p. 1079–1088. DOI 10.1016/j.jece.2017.01.032.

Shen F., Liu J., Zhang Z., Dong Y., Gu C. 2018. Density functional study of hydrogen sulfide adsorption mechanism on activated carbon. Fuel Processing Technology. Vol. 171 p. 258–264. DOI 10.1016/j.fuproc.2017.11.026.

Solisio C., Al Arni S., Converti A. 2019. Adsorption of inorganic mercury from aqueous solutions onto dry biomass of *Chlorella vulgaris*: kinetic and isotherm study. Environmental Technology (United Kingdom). Vol. 40(5) p. 664–672. DOI 10.1080/09593330.2017.1400114.

Tejada C., Herrera A., Ruiz E. 2016. Kinetic and isotherms of biosorption of Hg(II) using citric acid treated residual materials. Ingenieria y Competividad. Vol. 18(1) p. 117–127.

Tejada-Tovar C., Villabona-Ortíz A., González-Delgado Á.D., Granados-Conde C., Jiménez-Villadiego M. 2019. Kinetics of mercury and nickel adsorption using chemically pretrated cocoa (*Theobroma cacao*) husk. Transactions of the ASABE. Vol. 62(2) p. 461–466. DOI 10.13031/trans.13133.

Villabona-Ortíz A., Tejada-Tovar C., Gonzalez-Delgado A. 2018. Application of cement-based solidification/stabilization technique for immobilizing lead and nickel ions after sorption-desorption cycles using cassava peels biomass. Indian Journal of Science and Technology. Vol. 11 p. 1–6.

Wan Q., Rao F., Song S., Morales-Estrella R., Xie X., Tong X. 2018. Chemical forms of lead immobilization in alkali-activated binders based on mine tailings. Cement and Concrete Composites. Vol. 92 p. 198–204. DOI 10.1016/J.CEMCONCOMP.2018.06.011.

Wang H., Shen H., Shen C., Li Y., Ying Z., Duan Y. 2019. Kinetics and mechanism study of mercury adsorption by activated carbon in wet oxy-fuel conditions. Energy and Fuels. Vol. 33(2) p. 1344–1353. DOI 10.1021/acs.energyfuels.8b03610.

Wang L., Hou D., Cao Y., Ok Y.S., Tack F.M.G., Rinklebe J., O'Connor D. 2020. Remediation of mercury contaminated soil, water, and air: A review of emerging materials and innovative technologies. Environment International. Vol. 134 p. 105281. DOI 10.1016/j.envint.2019.105281.

Wang Y.T., Chen H., Wang D.J., Bai L.J., Xu H., Wang W.X. 2016. Preparation of corn stalk-based adsorbents and their specific application in metal ions adsorption. Chemical Papers. Vol. 70(9) p. 1171–1184. DOI 10.1515/chempap-2016-0064.

WHO 2003. Mercury in drinking-water background document for development of WHO Guidelines for Drinking-water Quality [online]. New York. World Health Organization pp. 10. Available at: https://www.who.int/docs/default-source/wash-documents/wash-chemicals/mercury-background-document.pdf?sfvrsn=9b117325_4

Zhang C., Sui J., Li J., Tang Y., Cai W. 2012. Efficient removal of heavy metal ions by thiol-functionalized superparamagnetic carbon nanotubes. Chemical Engineering Journal. Vol. 210 p. 45–52. DOI 10.1016/J.CEJ.2012.08.062.

Zhao R., Jia L., Yao Y.X., Huo R.P., Qiao X.L., Fan B.G. 2019. Study of the effect of adsorption temperature on elemental mercury removal performance of iron-based modified biochar. Energy and Fuels. Vol. 33(11) p. 11408–11419. DOI 10.1021/acs.energyfuels.9b02468.

Zhou Q., Duan Y., Chen M., Liu M., Lu P. 2017. Studies on mercury adsorption species and equilibrium on activated carbon surface. Energy and Fuels. Vol. 31(12) p. 14211–14218. DOI 10.1021/acs.energyfuels.7b02699.